Bulletin de la Société belge de Géologie, T. 101 (3-4), 1992, pp. 139-151.
Bulletin van de Belgische Vereniging voor Geologie. Ed. 1993

A NOTEWORTHY FRAGMENT OF THE SANTA CATHARINA METEORITE RECOVERED FROM A BELGIAN MUSEUM COLLECTION

by

R. VAN TASSEL[1], H. DILLEN[2], R. VOCHTEN[3], E. DE GRAVE[4] & J. HERTOGEN[5]

ABSTRACT

An irregular mass of about 28 kg, told to be a meteorite, but without any identification, has been recovered from a university collection in Antwerp, Belgium, and examined. Optical methods, scanning-electron-microscopy, X-ray spectrometry, X-ray diffraction, atomic absorption-spectroscopy, neutron activation analysis and Mössbauer spectroscopy are applied. Taenite, together with tetrataenite, troilite, magnetite, schreibersite and a ferrous phosphate are identified. According to its structure and composition the mass undoubtedly is a fragment of a Ni-rich iron meteorite and in any respect identical with the Santa Catharina ataxite. It ranks among the largest monolithic masses of this meteorite preserved in world collections.

KEYWORDS

Santa Catharina meteorite, Belgian collection, mineralogy, chemical composition, trace elements, Mössbauer spectroscopy.

1. INTRODUCTION

A rough, formless rusty-brown mass of about 28 kg was acquired, by the "Rijksuniversitair Centrum Antwerpen" (RUCA) in 1965, when the "Institut supérieur de Commerce de l'Etat d'Anvers (ISCEA) - Rijkshandelshogeschool van Antwerpen" was integrated in a larger department "Faculteit van Toegepaste Economische Wetenschappen" (RUCA).

The collection item was found without any documentation whatsoever ; but there were rumors that the heavy mass was a meteorite. It seemed scientifically justified to verify its true nature, in particular because the presence of a meteorite is rather surprising in an institute for economics. The "Institut supérieur de Commerce d'Anvers" was created in 1852 and from the early beginning (1853) a museum ("Musée de Produits commerçables") was established. Acquisitions were carefully registered, from 1853 to 1903, and were later on published in the printed "Annuaires" from 1904 to 1914. During World War I the institute was closed and no further details have been given in later annals.
In the course of the investigation it was found that the so-called meteorite had a very high Ni-content and peculiar structure. From a literature search (Buchwald, 1975, Graham *et al.* 1985) on Ni-rich iron meteorites, it became more and more probable that the mass could be a fragment of the Brazilian Santa Catharina iron meteorite, found in 1875. From this meteorite, large amounts (tons or hundreds of kg according to different authors) have been shipped to Europe for nickel extraction.

[1] Koninklijk Belgisch Instituut voor Natuurwetenschappen, Vautierstraat 29 - B-1040 Brussel.

[2] Research Centre for Application of Steel, OCAS - B-9060 Zelzate.

[3] Laboratorium voor Chemische en Fysische Mineralogie, Rijksuniversitair Centrum, Middelheimlaan 1 - B-2020 Antwerpen.

[4] Research Director, National Fund for Scientific Research (NFWO), Laboratorium voor Magnetisme, Universiteit Gent, Proeftuinstraat 86 - B-9000 Gent.

[5] Afdeling Fysico-chemische geologie, Laboratorium voor Geochemie, Universiteit Leuven, Celestijnenlaan 200C - B-3001 Heverlee

Particular attention was paid to every entry in the records of ISCEA, that could be an indication for the acquisition of a meteorite or a nickel ore from Brazil. Notwithstanding every effort, no mention of the subject was found in any extant records. It has also been supposed that the meteorite could have been acquired by ISCEA in 1930, when the Pavilion of Brazil was closed at the end of the International Exhibition in Antwerp, but a search in this direction remained fruitless as well.

2. MORPHOLOGICAL AND PHYSICAL CHARACTERISTICS

The surface of the 28 kg heavy, irregular mass (largest dimensions : 20 x 25 x 30 cm) (Plate 1, figs 1, 2, 3), is very oneven and has a redbrown-rusty colour. One obscure thumblike hollow can be seen (it may be the boundary of a troilite (FeS) vein (chap. 4.2), but the most striking feature is some cubic pattern of apparent cleavage directions. Filing on these spots immediately discloses a white-reflecting, bright metallic phase.

Detaching of specimens is not very easy as the mass is rather ductile. Nevertheless it shows some brittleness as it may break down along small cracks or troilite veins. Small fragments generally have some cubic or prismatic outline due to cleavage and are often covered with a black or brown thin crust. This crust is composed of magnetite with some iron-bearing weathering products wherein goethite has been recognized. Some greenish powder spots at the surface may be due to secondary Ni-bearing minerals. No sign of any technical treatment for nickel extraction was observed.

A cut of the mass in two nearly equal parts, disclosed very instructive surfaces (Plate 1, fig.4). Bright metallic patches of about 5-6 cm (called "grains" by Buchwald, 1975, p.1070) are surrounded by an irregular set of veins, which crisscross the whole mass and which are composed of a dull bronze-reflecting material, identified as troilite (chap. 4.2). These veins generally are 1-2 mm thick, exceptionally up to 1 cm and even thicker.

The bulk density of the whole mass is 6.30. The densities of the halves are 6.24 and 6.38 respectively, which indicates that both have grossly equal compositions.

The white-reflecting metallic areas are easy to polish and give evidence, as can already be seen with a magnifier, of some aligned and even crossing structure, whose orientation seems almost constant within an individual metallic patch. This structure is due to the presence of Fe-Ni-alloys of different compositions : taenite (Fe, Ni with Ni > 25 %) and oxygen-bearing zones with tetrataenite (ordered FeNi) (chap. 4.1). The metallic parts are traversed by many narrow cracks, sometimes irregular, but mostly showing some cubic pattern. These cracks are filled with magnetite (chap. 4.5).

Metallic fragments cleaned by filing from adhering crust, generally have densities between 7.0 and 8.2, mean value 7.4. The variable density is due to a heterogeneous distribution of cracks or of troilite or schreibersite $(Fe,Ni)_3P$ inclusions (chap. 4.2). The heaviest isolated metallic fragment (0.7 g) has a density of 8.8 and is composed of taenite with $\sim$ 66% Fe and $\sim$ 34% Ni (chap. 4.1).

Bronze-yellow reflecting fragments (0.3-0.5 g) from the swelling veins, also cleaned by filing, consist of troilite (chap. 4.2).

3. ANALYTICAL PROCEDURES

Visual observations were made under the optical ore microscope and the scanning electron microscope (SEM) equiped with detectors for secondary and back scattered electrons (BSE).

Most analytical data were obtained with an energy dispersive X-ray spectrometer (EDX). For oxygen detection a wavelength dispersive X-ray spectrometer (WDX) was used. Whenever possible the X-ray analyses were performed on flat polished surfaces, in some cases etched with diluted nitric acid.

The data are based on a standardless procedure with ZAF-correction. Elemental distribution mapping was performed in many cases for Fe, Ni, S, P and O.

Other analytical data, by atomic absorption spectrophotometry (AAS), or by classical redox titration (RT) for iron, were obtained on solutions after treatment of the sample with boiling concentrated nitric acid. Only a very small fraction (< 0.1 %) remained insoluble (magnetite according to X-ray powder diffraction).

Neutron activation analyses (NAA) were performed for Fe, Co, As, Au and Ir, on a 2 g sample obtained by filing from a fresh metallic surface. Two aliquots (415 mg and 290 mg) and standards were irradiated for 7 hrs at a thermal neutron flux of 2.10^{12} neutrons.cm^{-2}.sec^{-1}. Standards were made by pipetting mono-element solutions on filter paper. Stock solutions were prepared from high-purity stoichiometric compounds.

	% Fe	% Ni	% Co	% Cu	ppm Ir	ppm As	ppm Au
Previous analyses of Santa Catharina							
- Guignet & Ozorio de Almeida, 1876 (very first analysis)	64	36	-	-	-	-	-
- Damour, 1877	63.69	33.97	1.48	-	-	-	-
- Dyakonova & Charitonova, 1963	65.66	33.69	0.66	0.14	-	-	-
- Fouché, Smales, 1966	-	-	-	-	-	-	3.6
- Cobb, 1967	-	38.5	0.53	0.15	<1	-	-
- Smales et al., 1967	-	-	-	0.085	-	30.7	-
- Wasson & Schaudy,1971	-	33.62	-	-	0.02	-	
- Crocket, 1972	-	-	-	-	0.049	-	-
- Willis & Wasson, 1981	-	-	-	-	-	33.0	-
- Ryan et al., 1990	-	-	-	-	0.03	44.0	5.2
Present study							
EDX, surface analysis	~64	~35	~0.3	-	-	-	-
AAS, aliquots from 5g fragment	65.3	33.6	0.70	0.15	-	-	-
RT, aliquots from 5g fragment	65.2	-	-	-	-	-	-
AAS, aliquots from 2g powder	-	34.5	-	-	-	-	-
NAA, aliquots from 2g powder	-	-	0.55	-	0.022	53	3.3

Table 1. Chemical composition.

Standardisation for Fe was based on the specific γ-activity of high-purity iron foils used to monitor neutron flux gradients. The induced γ-activity was measured with a high resolution Ge(Li)-spectrometer at various time-intervals after irradiation.

The γ-activity of Ge, Ga, Os and Ir radioisotopes was completely masked by ^{59}Fe, ^{58}Co (from Ni) and ^{60}Co. After completion of the whole sample countings for a determination of Co, As and Au, a radiochemically pure Ir-fraction was isolated by standard radiochemical procedures to count ^{192}Ir (74 days). The two activated samples and the Ir-standard were dissolved in aqua regia in the presence of 2 mg Ir-carrier. After evaporation, the residue was taken up in 3.5 M HCl (+ ceric sulphate) and passed on a small anion-exchange column (Dowex 1X8 resin). The interfering elements Co and Fe were eluted with 3.5 M and 0.5 M HCl. The chloroiridate complex remains strongly adsorbed on the resin under these conditions. The upper 2 cm of the resin bed were removed and homogenized for counting with a Ge(-Li)-spectrometer. X-ray powder diffraction (XRD) was performed with a Debye-Scherrer camera (∅ 115 mm), using Mn-filtered Fe-radiation, at 40 kV and 20mA. The d_{hkl} of the diffraction lines were visually measured (± 0.1 mm) on the photographic film, without standard or shrinkage corrections, and their intensities were estimated visually (s : strong, m : medium, w : weak, v : very, d : diffuse).

Transmission ^{57}Fe-Mössbauer spectroscopy was applied at room temperature (300 K) on a thin slice (0.05 mm) of the metallic phase.

4. MINERALOGICAL COMPOSITION

4.1. Metallic phase

Metallic fragments were isolated for chemical analysis from cut surfaces and carefully cleaned as much as possible from adhering magnetite, weathering products or troilite by filing. A bulk surface analysis of the metallic phase was performed by EDX with ZAF-correction. Table 1 summarizes the results of the analyses which all point to a taenite composition, and compares them with the available

Present study		JCPD 23-297
2.07 Å	vs	2.08 Å (10)
1.79	m	1.80 (8)
1.27	mw d	1.27 (5)
1.08	m d	1.08 (8)
1.035	vw d	1.04 (5)

Table 2. X-ray data for taenite.

data recorded for the Santa Catharina meteorite.

X-ray powder diffraction was applied on powder, prepared by filing from polished metallic sections, and yielded the data given in Table 2, which agree with taenite.

Polished sections disclose quite remarkable features, as seen under the optical and the electron microscopes. Both techniques reveal that the surface of the metallic phase is heterogeneous, disclosing bright reflecting smooth areas, and mottled, somewhat darker areas (Plate 2, fig.1) The latter areas generally show more or less perfectly lined-up bands (Plate 2, figs 1 and 2), studded with specks (~ 5-30 µm), in a matrix of brighter material. The alignment of the dark bands is more or less constant throughout a whole metallic patch or grain, and remains unaffected by the cutting of the narrow magnetite veinlets. In a metallic zone (2.8 x 4.3 cm), devoid of troilite veins, the orientation of the mottled zones showed a faint inclination (7-8°) from one side to the other. These alignments show cross-cutting at an angle variable between ~ 90° and ~ 120°, presumably depending on the orientation of the polished section (Plate 2, fig.2). This structure, apparently continuous throughout the cut halves of the mass, should not be mistaken for a Widmanstätten pattern (kamacite α Fe-Ni intergrown with taenite γ Fe-Ni), as it is merely due to differences in taenite compositions (~ 35 % Ni and ~ 50 % Ni), subsequently emphasized when the sections are examined at high magnification. With respect to the Santa Catharina meteorite it has been reported (Buchwald 1975, p. 1070), that "polished sections through the metallic cores reveal an ataxitic structure with no trace of Widmanstätten precipitation, even at high magnification".

Etching of polished surfaces, with diluted alcoholic solutions of HNO_3 (10% or less), amplifies the already observed features or displays complementary information. The smooth areas remain apparently unaltered (Fe, Ni composition summed to 100 : ~65 % Fe, ~35 % Ni by EDX), but the mottled areas (Fe, Ni composition : ~50 % Fe, ~50 % Ni by EDX), more readily etched, turn blackish, and their peculiar surface structure becomes very obvious with alignments now quite more visible (Plate 2, fig.3). Included schreibersite (Plate 2, fig. 3) is apparently not affected by the etching procedure and is, in this way, easily recognized due to its high white-reflecting power under the ore microscope. It is very striking that the mottled areas do not occur in the neighbourhood of schreibersite.

High magnification SEM-views reveal that the nature of the apparently smooth areas and of the mottled areas is rather complex. After etching, the former areas show a parquet-like structure of tiny blocs (4-12 µm) set, according to a cubic (Plate 2, fig.4) or lozenge pattern (depending on the orientation of the section), in a network of very fine threads (2 µm). The heterogeneous nature observed on microscale is characterized by differences in chemical composition.

According to EDX the parquet-blocs, in the smooth areas, have the same composition (~67 % Fe, ~33 % Ni) as the network itself. The specks (Plate 2, figs 5 and 6), in the darker areas, are oxygen-bearing (several percent of oxygen by WDX), and have a Fe-Ni-composition (summed to 100) of ~50 % Fe,~50 % Ni.

Results of transmission ^{57}Fe-Mössbauer spectroscopy on a 0.05 mm thin metal slice, at 300 K, are illustrated in figure 1 : the spectrum could numerically be interpreted as a superposition of two magnetic sextet subspectra and a non-split central line. The metallic phase is composed of 45 % of a γ Fe-Ni phase with ≈ 28 % Ni (central peak, hyperfine field H_{nf}=0), 30 % of an ordered 50 % Fe-50 % Ni-alloy (tetrataenite) (dotted line, H_{nf}=287 kOe) and 25 % of a partly disordered 50 % Fe-50 % Ni-alloy (full line, H_{nf}=298 kOe) (De Grave *et al.*, 1992).

4.2. Troilite FeS

This mineral forms the numerous irregularly curved veins, of variable thickness (1-10 mm, and even more), crisscrossing the whole meteorite (Plate 1, fig. 4). It separates the cm-sized taenite grains and is partly esponsible for the brittleness of the meteorite, breaking along the metal-troilite boundaries. Troilite is difficult to polish, has a bronze-reflecting power, and sometimes encludes magnetite. Isolated fragments (0.3-0.5 g), cleaned by filing, have densities between 4.9 and 5.5, mean value 5.2 (pure troilite has d=4.79). Analyses on 0.3 g by redox titration gave 68.7% Fe and by AAS 67,2% Fe and only traces of Ni (<0.02%). EDX on several points yielded ~69 % Fe, ~31 % S and very small amounts of Ni (less than 1 %), to be compared with 63.6 % Fe and 36.4 % S in stoichiometric FeS. The XRD-data (Table 3) agree with the standard-file

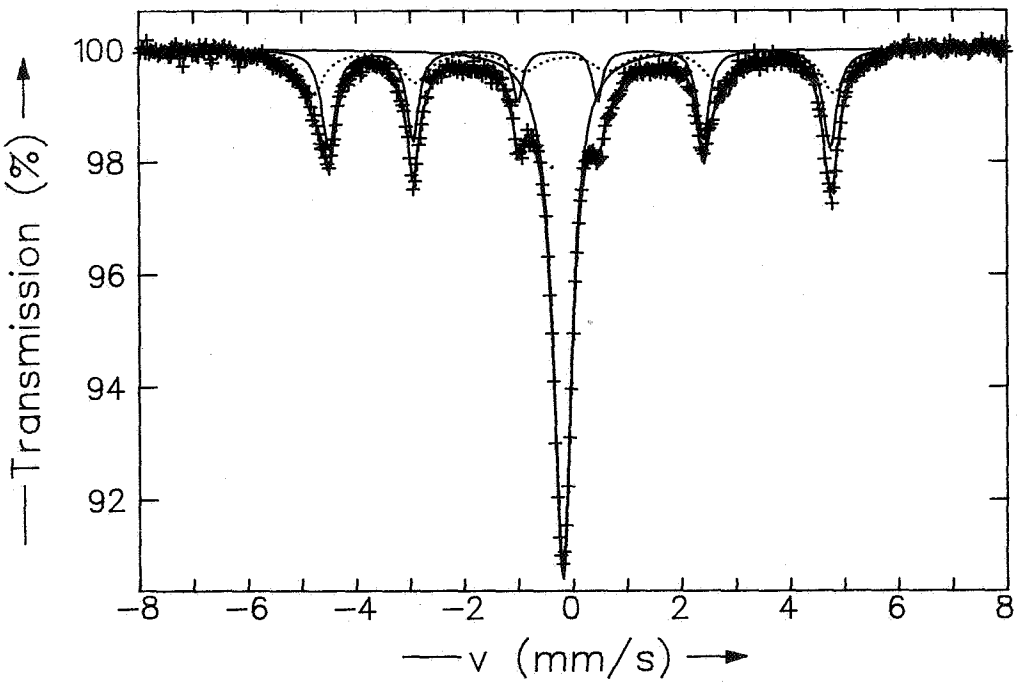

Figure 1. - ^{57}Fe-Mössbauer absorption spectra of a thin slice (0.05 mm) of the metal phase.

Present study		JCPD 11-151	Present study		JCPD 11-151
5.2 Å	vw	5.4 Å (20)	1.503	vw	-
4.76	vw	4.74 (10)	1.484	vw	-
4.12	vw	-	1.47	w	1.469 (30)
2.98	ms	2.98 (40)	1.33	m	1.331 (40)
2.66	s	2.66 (40)	1.318	w	-
2.52	m	2.52 (10)	1.283	vw	1.284 (5)
2.15	vw	2.14 (10)	1.229	vw	1.224 (20)
2.09	vs	2.09 (100)	1.118	m	1.119 (40)
1.91	w	1.923 (30)	1.105	w	1.108 (30)
1.744	vw	1.748 (10)	1.093	w d	1.091 (10)
1.638	w	1.634 (30)	0.993	vw d	0.994 (20)
1.612	vw	1.595 (5)			

Table 3. X-ray data for troilite.

card for troilite and the occurrence of the lines 2.52,2.09, 1.47 and 1.12 Å seems quite valuable for the distinction troilite/pyrrhotite, while the line 2.06 Å seems more characteristic for pyrrhotite.

4.3 Schreibersite, $(Fe,Ni)_3P$

This mineral mostly occurs enclosed in the metallic phase. It can easily be recognized in etched polished surfaces, owing to its resistance to etching and its high reflecting power. It occurs as tiny needles or spindles (rhabdite) (20-40 x 60-400 µm) (Plate 2, fig. 2), crystals (Plate 2, fig. 7) or mm-sized laths (Plate 2, fig. 3). Sometimes the schreibersite crystals are X-shaped and may have a nucleus or an adhering grain (80-350 µm) of iron phosphate (Plate 2, fig. 8) (chap. 4.4). The larger crystals mostly show irregular cracks (Plate 2, figs 3 and 8 ; Plate 3, fig. 4). According to many point analyses by EDX the composition is ~53 % Fe, ~35 % Ni and ~12 % P. The XRD-data fully agree with those for schreibersite (Table 4).

4.4. Iron phosphate

Under the reflecting microscope deep-grey rounded or subangular grains (80-350 µm) are seen enclosed in often X-shaped schreibersite or are in touch with it (Plate 2, fig.8). These inclusions are oxygen-bearing according to WDX and are composed (EDX) of ~66 % FeO and ~34 % P_2O_5 calculated as oxides. Ni, Mn and Si were only observed as traces. These characteristics strongly point to a ferrous phosphate mineral $Fe_3(PO_4)_2$, endmember of the graftonite-sarcopside group which ideally contains 60.3 % FeO and 39.7 % P_2O_5.

Present study		JCPD 16-707	Present study		JCPD 16-707
2.99 Å	vw	2.98 Å (?) ≈ kamacite-troilite	1.676	w	1.682 (25)
2.49	w	2.50 (25)	1.406	vw	-
2.19	vs	2.19 (100)	1.280	w	1.274 (30)
2.13	m	2.13 (50)	1.228	w	1.234 (14)
2.11	m	2.11 (70)	1.204	vw	1.205 (14)
2.02	m	2.02 (50)	1.193	vw	-
1.97	s	1.972 (70)	1.148	w	1.153 (10)
1.832	w	1.823 (25)	1.122	vw	-
1.773	w	1.778 (25)	1.115	vw	1.110 (10)
1.758	x	1.762 (35)	1.107	w	-
			1.095	w	1.097 (25)

Table 4. X-ray data for schreibersite.

Present study		JCPD 19-629	Present study		JCPD 19-629
4.86 Å	w	4.85 Å (8)	1.486	s	1.485 (40)
4.19	vw	-	1.330	w	-
2.97	ms	2.97 (30)	1.281	w	1.281 (10)
2.65	vw	-	1.266	vw	1.266 (4)
2.53	vs	2.532 (100)	1.212	w	1.212 (2)
2.43	w	-	1.124	w	1.122 (4)
2.098	ms	2.099 (20)	1.093	m	1.093 (12)
1.712	w	1.715 (10)	1.051	mw	1.050 (6)
1.611	ms	1.616 (30)	0.990	w	0.989 (2)

Table 5. X-ray data for magnetite.

The occurrence of iron phosphate in the Santa Catharina meteorite has been noticed for the first time by Clarke (1984). Zhang *et al.* (1990) have observed over 50 individual phosphate crystals, several 0.5 mm long, occurring within troilite or schreibersite, or at the boundaries between troilite, schreibersite or metal. Electron microprobe analysis of 25 crystals yielded 60.0 ± 0.5 % FeO and 40.3 ± 0.5 % P_2O_5.

Buchwald (1975), in his monumental "Handbook of Iron Meteorites", reported and showed phosphate inclusions for the Wiley octahedrite as "phosphate crystal" (~40 µm) in X-shaped schreibersite (Buchwald, 1975, p.1309, fig.1936), as "phosphate crystal" (~60 µm) in schreibersite (p.1310), as "angular phosphate crystal" (~75 µm) in schreibersite (p.1311) and as "phosphate" (25 µm) according to the sequence : phosphate, troilite, schreibersite, and kamacite (p.122). A description for the same meteorite is stated as follows : "a number of rounded or subangular phosphate inclusions, typically 20-100 µm in size and deep gray in reflected light occur evenly distributed" and electron microprobe revealed "Fe, Mn, P and O, corresponding to sarcopside or graftonite" (p.1311). Grains with similar characteristics in the Santa Catharina meteorite were not identified as a phosphate phase. Indeed, Buchwald (1975) reported that a "silicate crystal (50 µm) upon which schreibersite has nucleated" (p.1071, fig.1526) and "accessory silicates in the form of 20-300 µm rounded and angular bodies, upon which phosphides have precipitated, occur irregularly in Santa Catharina" (p.1071). Furthermore, a similar angular grain (100 µm), surrounded by a wide rim of brecciated schreibersite, is seen as a "silicate (?) crystal" (p.1248, fig.1821) in the Ni-rich Twin City ataxite.

4.5 Magnetite

This mineral fills the numerous, narrow, frequently perpendicular cracks traversing the metallic phase or cementing fragments of metal (Plate 3, fig.1). In some instances the thin crust at the boundary of the metal exhibits well developed magnetite microcrystals (15-150 µm) (Plate 3, fig.3). The mineral sometimes includes brecciated fragments of schreibersite or of an unidentified nickel sulphide and also occurs as inclusion in troilite veins . It is very resistant to chemical attack. Even boiling in concentrated HNO_3, though dissolving metallic and troilite fragments, leaves magnetite grains unaltered. Elemental distribution mapping revealed that the mineral is Ni-free (Plate 3, fig.2). XRD proved its identity with standard magnetite (Table 5).

4.6 Unidentified sulphides

Peculiar inclusions of quite complex mineralogical composition were found within taenite. In one case (Plate 3, fig.4) an oval, apparently broken grain (0.15 mm) shows in its interior an iron sulphide (? troilite) embedded in a Fe-Ni-sulphide (? pentlandite), and is further surrounded by nickel sulphide; the whole assemblage is bordered by a 9-45 µm thick rim of cracked schreibersite (Plate 3, figs. 5,6,7 and 8).

As reported in chap. 4.5, Ni-rich (~78 % Ni) brecciated sulphide grains (5-20 µm) occur embedded in magnetite.

5. Conclusion

All the described characteristics of the examined meteorite allow to identifiy it as a fragment of the Santa Catharina Ni-rich ataxite, Brazil, found in 1875. Its weathered appearance, main mineralogical composition (taenite and tetrataenite), structure emphasized by curved veins of troilite (figured in Meunier, 1884 ; Brezina, 1896), chemical composition (very high Ni-content (~35 %) of the bulk metallic phase), occurrence of 50 % Fe -50 % Ni-alloy, content of the trace elements (As, Au and Ir), all match very well the data recorded and summarized by Buchwald (1975), or later reported by Albertsen *et al.* (1978), Danon *et al.* (1979, 1980,1985), Zhang *et al.* (1990), Miller *et al.* (1992).

The presence of a meteorite once considered a nickel ore in a museum of commercial goods is understandable. But the way along which this meteoritic fragment ended up in the "Institut supérieur de Commerce d'Anvers" remains obscure, in spite of plenty inquiries and investigations in records.

The meteorite is stored in the collection of the "Dienst voor Delfstofkunde, Aardkunde en Fysische Aardrijkskunde, Faculteit Wetenschappen, Rijksuniversitair Centrum Antwerpen" with the register number 658. It is quite an interesting collection specimen, as it seems to rank among the largest (after Rio de Janeiro, Paris, Vienna, Chicago) recorded monolithic masses, preserved in collections (Buchwald 1975, Brezina, 1896, Graham *et al.*, 1985).

6. ACKNOWLEDGEMENTS

Thanks are due to Prof.Dr.W. De Breuck, RUCA, for permission to examine the meteorite; to the Staff of the Meteorite Department, Musée National d'Histoire Naturelle, Paris, for providing references, advice and visiting facilities; to Mr. K. Van Springel for technical assistance; to Prof. em. V. da Fonseca, ISCEA; to the Stadsarchief of Antwerp; to the Embassy of Brazil, Cultural Department, Brussels, for help in finding potential information sources with respect to the mode of acquisition by ISCEA; and to Mrs. D. Dielen for typing the manuscript.

7. REFERENCES

ALBERTSEN, J.F., JENSEN, G.B. & KNUDSEN, J.M., 1978 - On superstructure in meteoritical taenite. *Meteoritics*, **13**: 379-383.

BILD, R.W., 1974 - New occurrences of phosphates in iron meteorites. *Contrib.Miner.Petrol.*, **45**: 91-98.

BOWLES, J.S., HATHERLY, M. & MALIN A.S., 1978 - FeNi-superlattice formation by corrosion of Santa Catherina meteorite. *Nature*, **276**: 168-169.

BREZINA, A., 1896 - Die Meteoritensammlung des k.k. naturhistorischen Hofmuseums am 1 Mai 1895. *Ann.k.k. Naturhist.Hofmuseums*, **10**.

BUCHWALD, V.F., 1975 - *Handbook of Iron Meteorites. Their history, composition and structures*, 3 vol., 1418 p. Univ.California Press, Berkeley.

BUCHWALD, V.F., 1977 - Mineralogy of Iron Meteorites. *Phil. Transact.roy.Soc.London, Math.Phys.Sci.*, **A286**: 453-491.

CLARKE, R.S.Jr.& SCOTT, E.R.D., 1980 - Tetrataenite - ordered FeNi, a new mineral in meteorites. *Amer.Miner.*, **65**: 624-630.

CLARKE, R.S., 1984 - Structural development in the Santa Catharina Meteorite. *Meteoritics*, **19**: 207-208.

COBB, J.C., 1967 - A trace-element study of iron meteorites. *J. Geophys.Res.*, **72**: 1329-1341.

CROCKET, J.H., 1972 - Some aspects of the geochemistry of Ru, Os, Ir and Pt in iron meteorites. *Geochim.Cosmochim. Acta*, **36**: 517-535.

DAMOUR, A., 1877 - Sur un fer métallique trouvé à Santa-Catharina (Brésil). *C.R. hebd.Acad.Sci.*, **84**: 478-481.

DANON, J., SCORZELLI, R., SOUZA AZEVEDO, I., CURVELLO, W., ALBERTSEN, J.F. & KNUDSEN, J.M., 1979 - Iron-nickel 50-50 superstructure in the Santa Catharina meteorite. *Nature*, **277**: 283-284.

DANON, J., SCORZELLI, R.B. & AZEVEDO, I.S., 1980 - Mössbauer studies of the Fe-Ni ordered phase (superstructure Ll 10) in meteorites. *J. Phys.*, **41/C1**: 363-364.

DANON, J., SCORZELLI, R.B. & GALVAO DA SILVA, E., 1985 - Microstructure of the Santa Catharina meteorite. *Meteoritics*, **20**: 632.

DE GRAVE, E., VANDENBERGHE, R.E., DE BAKKER, P.M.A., VAN ALBOOM A., VOCHTEN R. & VAN TASSEL R., 1992 - Temperature dependance of the Mössbauer parameters of the Fe-Ni-phases in the Santa Catharina meteorite. *Hyperfine Interactions*, **70**: 1009-1012.

DYAKONOVA, M.I. & CHARITONOVA V.Y., 1963. Chemical analyses of different meteoritic irons. *Meteoritika*, **23**: 43-44 (in Russian).

FOUCHE, K.F. & SMALES, A.A. 1966 - The distribution of gold and rhenium in iron meteorites. *Chem. Geol.*, **1**: 329-339.

GRAHAM, A.L., BEVAN A.W.R. & HUTCHISON R., 1985 - Catalogue of Meteorites. 460 p. *British Museum (Nat.Hist.)*, London.

GUIGNET, E. & OZORIO DE ALMEIDA, G., 1876 - Sur un fer météorique très-riche en nickel, trouvé dans la province de Santa-Catharina (Brésil). *C.R. hebd.Acad.Sci.*, **83**: 917-918.

KVASHA, L.G., KOLOMENSKII, V.D. & BUDKO, I.A., 1969 - Struktura nikelistovo zheleza i sulfid meteorita Santa Catharina (Structure du fer nickelé et des sulfures de la météorite Santa Catharina). *Meteoritika*, **29**: 68-75 (in Russian).

MEUNIER, S., 1884 - Météorites. *In* : Encyclopédie chimique. II. Métalloïdes, 102-108, 501-502. Dunod, Paris.

MILLER, M.K. & RUSSELL, K.F., 1992 - An APFIM investigation of a weathered region of the Santa Catharina meteorite. *Surface Science*, **266**: 441-445.

RYAN D.E., HOLZBECHER J. & BROOKS R.R., 1990 - Rhodium and osmium in iron meteorites. *Chem. Geol.*, **85**: 295-303.

SMALES, A.A., DAPPER, D. & FOUCHE, K.F., 1967 - The distribution of some trace elements in iron meteorites, as determined by neutron activition. *Geochim.Cosmochim. Acta*, **31**: 673-720.

WASSON, J.T. & SCHAUDY, R., 1971 - The chemical classification of iron meteorites. - V. Groups III C and III D and other irons with germanium concentrations between 1 and 25 ppm. *Icarus*, **14**: 59-70.

WILLIS, J. & WASSON J.T., 1981 - Instrumental Neutron Activation Analysis of Iron Meteorites. *Radiochem. Acta*, **29**: 45-51.

WULFING, E.A., 1897 - *Die Meteoriten in Sammlungen und ihre Literatur*. 461 pp., Laub, Tübingen.

ZHANG, J., WILLIAMS, D.B., GOLDSTEIN, J.I. & CLARKE R.S. Jr, 1990 - Electron microscopy study of the iron meteorite Santa Catharina. *Meteoritics*, **25**: 167-175.

Manuscript received on 9.11.1992 and accepted for publication on 15.03.1993.

PLATE 1

Figures 1, 2 and 3. Views of the irregular 28 kg meteoritic mass (~20x25x30cm).

Figure 4. Polished surface of a section through the centre of the meteoritic mass, showing metal patches ("grains") with light and dark areas, crisscrossing and swelling troilite viens, and plenty of narrow, approximatively perpendicular cracks filled with magnetite. Inclined view. Scale bar (foreground) 5 cm.

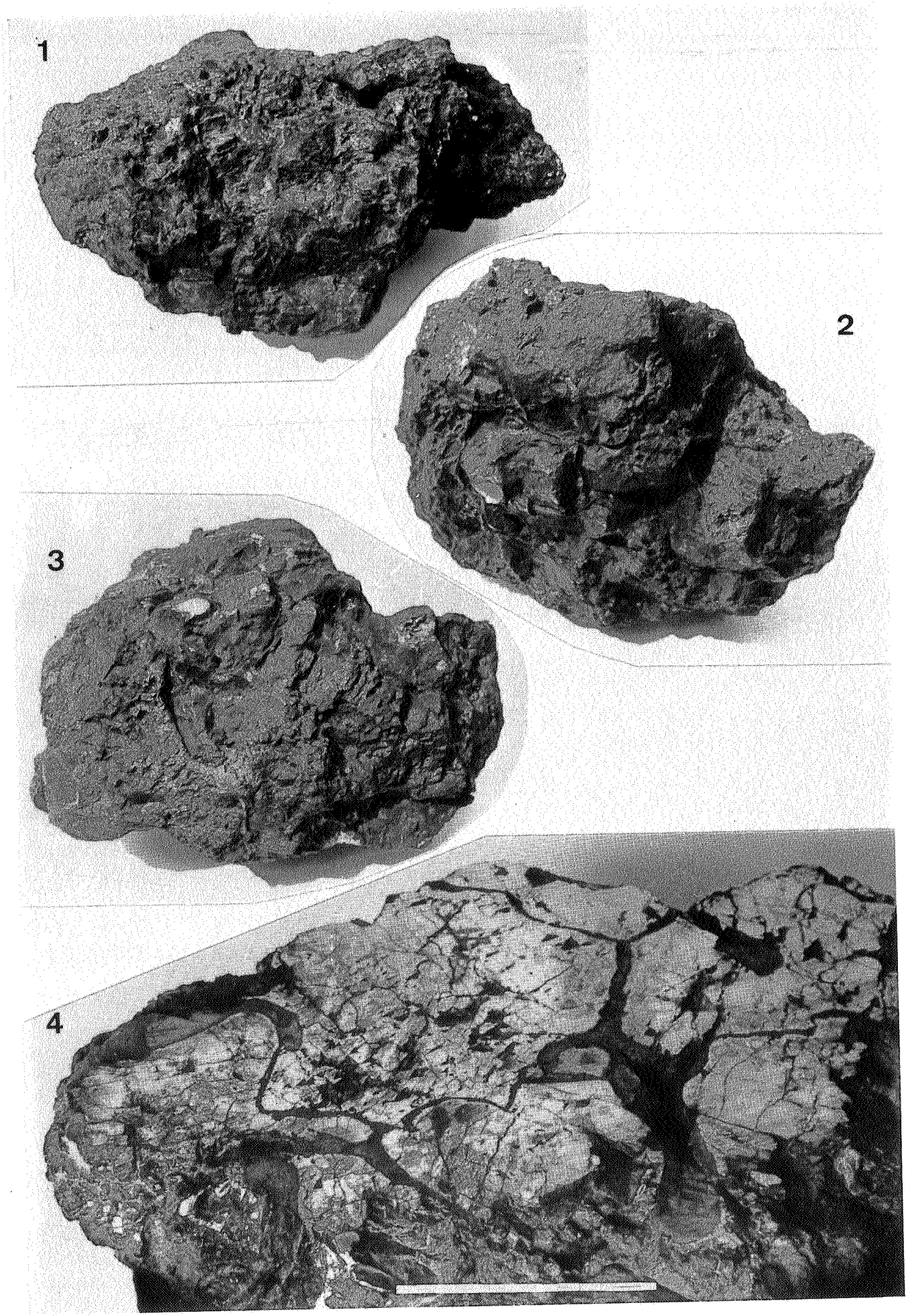
1
2
3
4

PLATE 2

Figure 1. Light and dark areas in the metal phase. The specks in the dark areas are clearly aligned. Etched polished section. BSE-image. Scale bar 1 mm.

Figure 2. Light and dark areas in the metal phase. Polished section. Scale bar 1 mm. On the right, within the light area, a spindle-like schreibersite inclusion occurs.

Figure 3. Light and dark areas in the metal phase surrounding laths of cracked schreibersite. The dark areas disappear in the neighbourhood of schreibersite. Etched polished section. Scale bar 1 mm.

Figure 4. Parquet-like structure of the light area in the metal phase. SEM-image. Etched polished section. Scale bar 0.1 mm.

Figures 5 and 6. Oxygen-bearing specks with ~50 % Fe : ~50 % Ni in the dark area of the metal phase. Polished section. BSE-image. Fig. 5: scale bar 0.1 mm, Fig. 6 : 0.01 mm.

Figure 7. Schreibersite crystal enclosed in taenite. Etched polished section. BSE-image. Scale bar 0.1 mm.

Figure 8. X-shaped schreibersite crystal, with iron phosphate nucleus, enclosed in taenite. Polished section. BSE-image. Scale bar 0.1 mm.


1
1mm300kV 408E1 0108/04 023


2
1mm300kV 655E1 0127/04 023


3
1mm300kV 276E1 0117/04 023

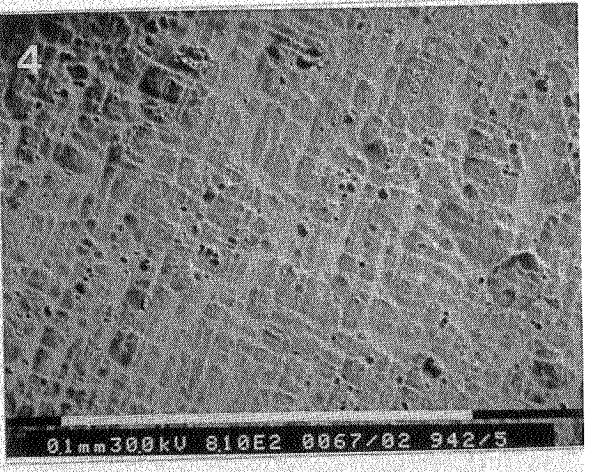
4
01mm300kV 810E2 0067/02 942/5

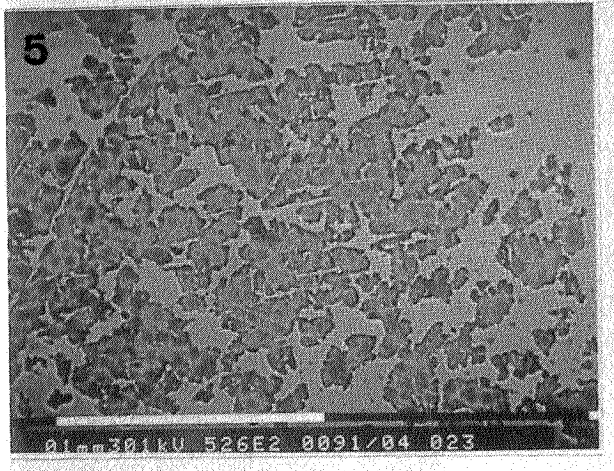
5
01mm301kV 526E2 0091/04 023

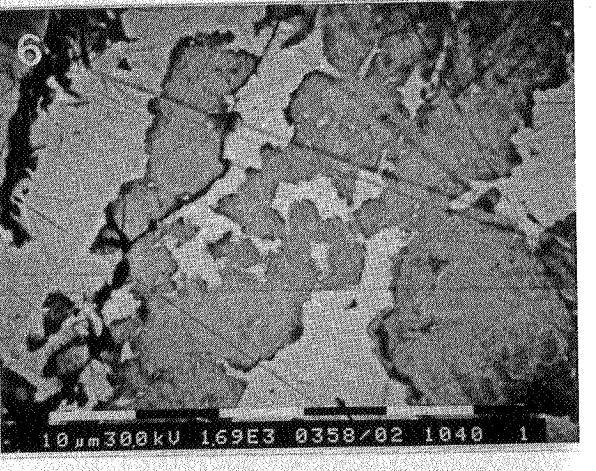
6
10µm300kV 169E3 0358/02 1040 1

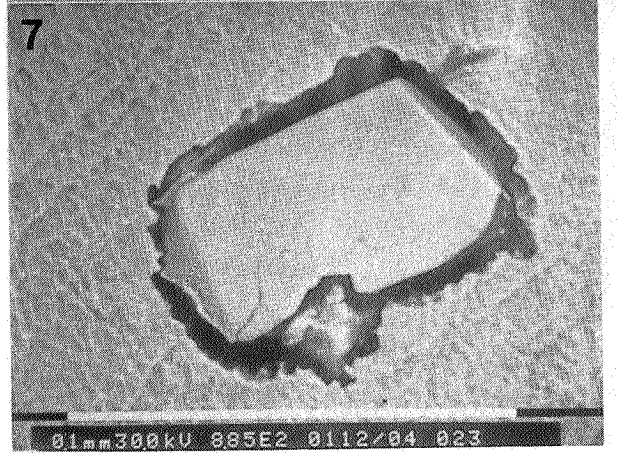
7
01mm300kV 885E2 0112/04 023


8
01mm301kV 462E2 1004/02 1098/D

PLATE 3

Figure 1. Magnetite filling cracks and cementing brecciated fragments of taenite in the metal phase. Polished section. BSE-image. Scale bar 0.1 mm.

Figure 2. Ni-distribution mapping of area in figure 1, showing Ni-free magnetite in taenite region. Scale bar 0.1 mm.

Figure 3. Magnetite microcrystals in rusty crust. SEM-image. Scale bar 0.1 mm.

Figure 4. Complex inclusion in the metal phase with nuclei of iron sulphide surrounded by Fe-Ni-sulphide, embedded in nickel sulphide and the whole in contact with cracked schreibersite. Etched polished section. BSE-image. Scale bar 0.1 mm.

Figures 5, 6, 7 and 8. Distribution maps of the area of figure 4 :
figure 5 : Fe ; figure 6 : Ni ; figure 7 : S ; figure 8 : P.

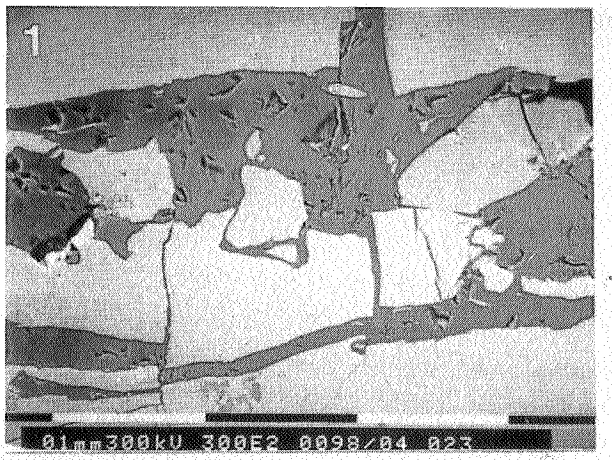
1
01mm300kV 300E2 0098/04 023

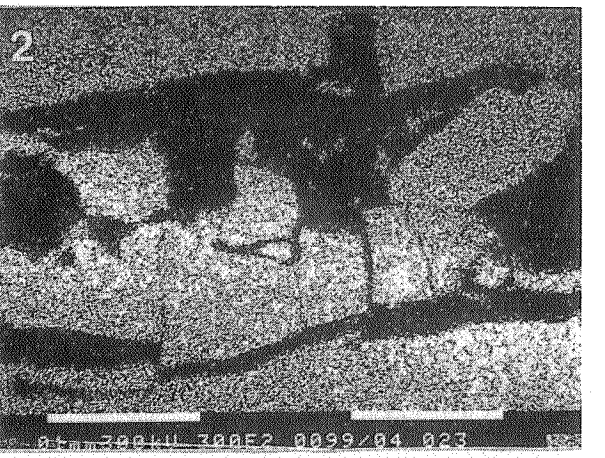
2
01mm300kV 300E2 0099/04 023

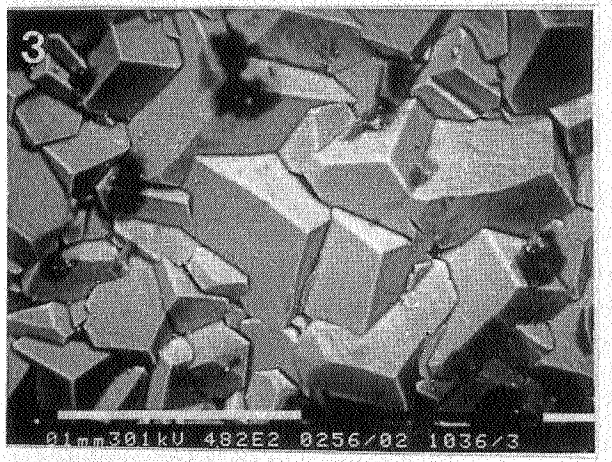
3
01mm301kV 482E2 0256/02 1036/3

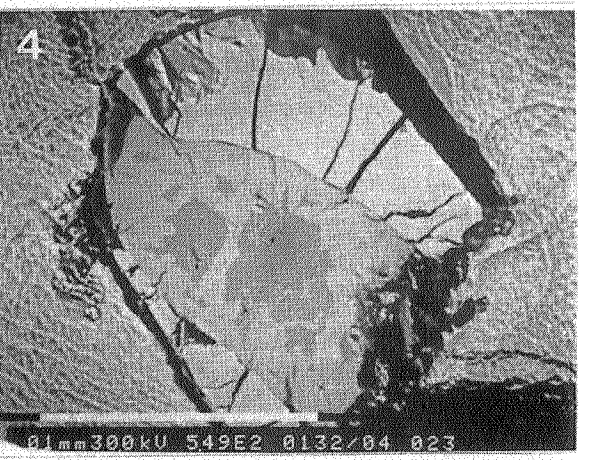
4
01mm300kV 549E2 0132/04 023

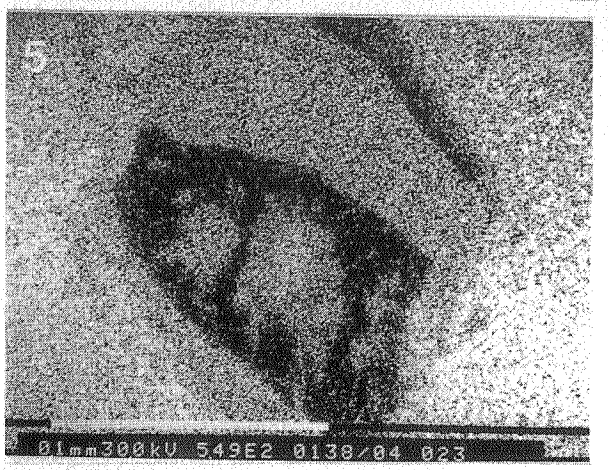
5
01mm300kV 549E2 0138/04 023

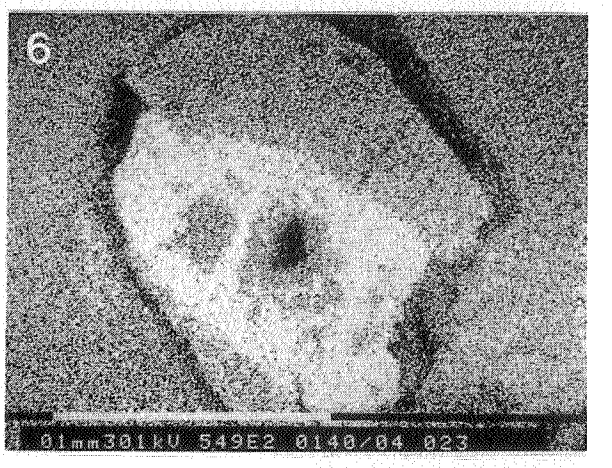
6
01mm301kV 549E2 0140/04 023

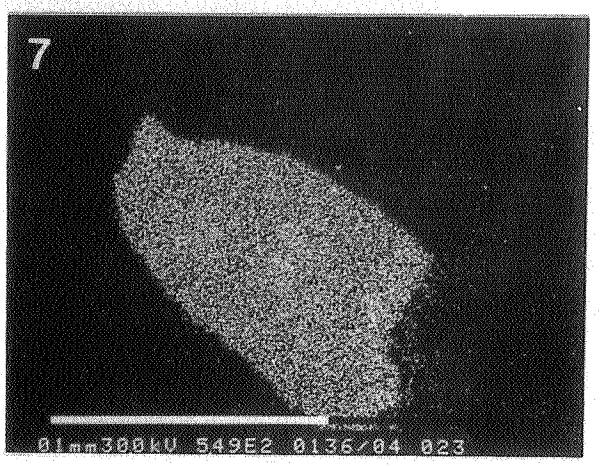
7
01mm300kV 549E2 0136/04 023

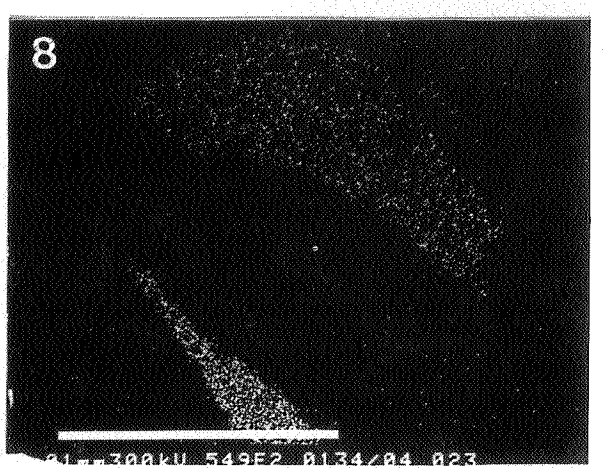
8